Mathematisch-Naturwissenschaftliche Fakultät

Markus Gühr

Ultrafast Soft X-ray Probing of Gas Phase Molecular Dynamics

Ultrafast Soft X-ray Probing of Gas Phase Molecular Dynamics

MARKUS GÜHR

Institut für Physik und Astronomie, Universität Potsdam, Potsdam, Germany and PULSE,
SLAC National Accelerator Laboratory, Menlo Park, CA, USA

Introduction

The molecular ability to selectively and efficiently convert sunlight into other forms of energy like heat, bond change, or charge separation is truly remarkable. The decisive steps in these transformations often happen on a femtosecond timescale and require transitions among different electronic states that violate the Born-Oppenheimer approximation (BOA) [1]. Non-BOA transitions pose challenges to both theory and experiment. From a theoretical point of view, excited state dynamics and nonadiabatic transitions both are difficult problems [2, 3] (see Figure 1(a)). However, the theory on non-BOA dynamics has advanced significantly over the last two decades. Full dynamical simulations for molecules of the size of nucleobases have been possible for a couple of years [4, 5] and allow predictions of experimental observables like photoelectron energy [6] or ion yield [7–9]. The availability of these calculations for isolated molecules has spurred new experimental efforts to develop methods that are sufficiently different from all optical techniques. For determination of transient molecular structure, femtosecond X-ray diffraction [10, 11] and electron diffraction [12] have been implemented on optically excited molecules.

Here, we concentrate on X-ray spectroscopic probes, which provide a new perspective on molecular photoenergy conversion because of their element and site specificity. The binding energy of core electrons is strongly dependent on the element, differing by about 100 eV for the neighbor elements of carbon, nitrogen, and oxygen. This allows for a separation of spectroscopic features from different elements within one molecule. Slight shifts in the binding energy of the same element result from the electronegativity of the nearest environment within the molecule. Those are used to distinguish different molecular sites of
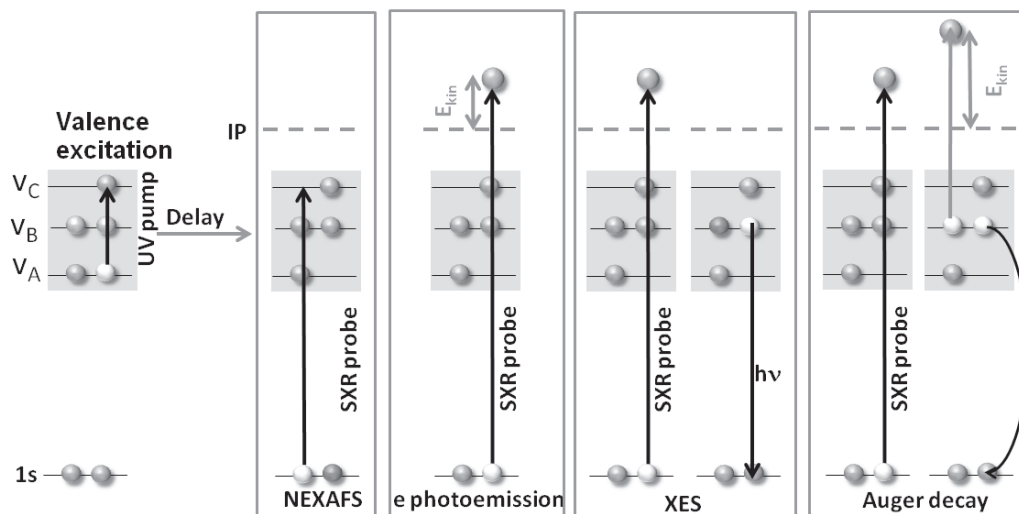

Figure 1: Comparison of different soft X-ray probes of molecular dynamics, presented in a single electron model. The molecular excitation occurs via a valence transition from orbital v_A to v_C, induced by an optical pulse. The valence electronic structure is probed by a delayed soft X-ray pulse. In near-edge X-ray absorption fine structure (NEXAFS) spectroscopy, one probes the valence occupation by resonant absorption from the core levels. In X-ray photoelectron emission (XPS), one directly analyzes the kinetic energy of the emitted core electron. In X-ray emission spectroscopy (XES), the core electron is promoted above the ionization limit and the emitted photons from valence electrons filling the core hole are spectrally resolved. In the soft X-ray region, photoemission is small; instead, the Auger emission sketched in the third field is the prominent process. In this technique, the kinetic energy of the Auger electrons is analyzed.

one particular element [13]. Furthermore, since core electrons are so strongly localized, they can be used to determine the localization of valence excited states in resonant absorption.

Since the invention of X-ray free electron lasers (FELs) [14–16], ultrashort X-ray pulses with unprecedented intensity are available to a large user community. The first experiments on optically excited molecules have concentrated on nucleobase photoprotection [17], excited state isomerization [18], and dissociation dynamics [19]. As X-ray FELs now come into their second phase with high-repetition-rate sources based on superconducting accelerators and seeded sources, exciting new possibilities arise for the molecular dynamics community.

Apart from FELs, strong-field high harmonic generation (HHG) of X-ray pulses is demonstrating rapid progress, which provides a complementary set of experiments based on a smaller laser laboratory infrastructure. This article will give a short overview of first experiments on gas phase molecular dynamics probed in the soft X-ray range and present opportunities arising as FEL and HHG sources progress.

Soft X-ray spectroscopic probing of molecular dynamics

Figure 1 presents different methodological approaches to study optically induced molecular dynamics using soft X-ray probing. All techniques rely on an optical pulse to excite molecular dynamics via a transition to a higher lying electronic state (for example, a transition from a orbital v_A to v_C in the figure). As the molecule undergoes changes to its geometry as well as electronic structure, it is probed by a time-delayed soft X-ray pulse that excites a 1s core electron.

If the core electron is excited above the ionization limit, its kinetic energy and amplitude can be determined as a function of pump probe delay. Photoelectron emission probing is sensitive on the binding energy and ionization probability as a function of the transiently changing molecular geometry and electronic structure. Both change the screening of the core hole and thus binding energy as well as dipole matrix element. Thus far, this technique has been tried once at a free electron laser [20], but suffers under the enormous spectral fluctuations in an FEL which starts lasing from noise by self-amplified spontaneous emission (SASE) [21].

Resonantly exciting the 1s core electron to valence orbitals leads to an X-ray absorption signature indicative of the valence electronic structure. In static spectroscopy, this method is rather powerful for determining the electronic structure of the ground state [22] and binding geometry to surfaces [23]. At current SASE sources, however, the technique suffers the same serious limitations as photoelectron emission, as it is directly sensitive on the FEL spectrum. To overcome this, a monochromator can be used for spectral filtering. Thereby, the spectral fluctuations are transformed into intensity noise, which facilitates the technique on cost of longer data acquisition time.

X-ray emission probing, in contrast, does not suffer this disadvantage. As long as the 1s core electron is excited, leaving behind a hole, the molecule undergoes core hole decay, independent of the initial FEL wavelength. The probability for radiative core hole decay, however, is small for light atoms; typically about 1 in 1000 excited molecules undergo this process, while the others decay via emission of an Auger electron. Furthermore, soft X-ray spectrometers, relying on grazing incidence reflection on a grating, have a small angular collection efficiency in the range of 2×10^{-5} and a detection efficiency of 5×10^{-2}. Assuming a gas density of 10^{14} cm^{-3}, which can be accomplished for nucleobases in heated cells, and an absorption cross-section around 1 Mbarn, we can detect one photon per 10^{14} incoming photons from the target. With current sources delivering about 10^{11} photons per pulse at 100 Hz to the interaction region, the acquisition times for time-resolved experiments are simply too large. On surfaces, however, first experiments have been performed [23]. Scaling the molecular density is, of course, possible for molecules that in gas form at room temperature. For larger molecules like nucleobases or aminoacids, higher densities in heated gas cells become increasingly difficult, as the high temperatures compromise sample stability and molecules tend to undergo chemical transformations and decomposition.

The core hole decay via Auger electrons is much more probable compared to emission. In addition, high-efficiency detectors are available for Auger electrons. Thus, the logical first experiment for probing molecular dynamics at FELs was a time-delayed soft X-ray Auger probing approach. Figure 1 shows a sketch of the Auger probing principle. A nonresonant X-ray pulse is used to create a 1s core hole on the molecule. The Auger decay involves two valence electrons. Since it starts with a confined core hole, those valence electrons show a high degree of localization at the core site. The selection of the Auger kinetic energy determines the core hole decay to be observed. The Auger kinetic energies are slightly lower than the core binding energies at the respective edge. For the oxygen core hole decay in thymine, we observe a several 10 eV wide spectrum with the strongest Auger yield around 500 eV shown in Figure 2(a). The Auger kinetic energy is independent of the photon energy; thus, the method is ideally suited for SASE FEL sources with their large spectral fluctuations.

Figure 2(a) shows a UV pump-X-ray probe scan of the nucleobase thymine. The most pronounced change occurs in the first picosecond. The subtraction of unexcited spectra from UV excited spectra in Figure 2(a) reveals the photoinduced molecular transformation. One can clearly identify a signal decrease in the kinetic energy region around 500 eV that lasts for the full measurement interval. A short-lived positive feature can be observed at 507 eV kinetic energy. A cut through the difference spectrum at short times is given in blue in Figure 2(c). Such a difference spectrum reflects a UV-induced shift of the whole ground state Auger band towards higher Auger kinetic energies. The immediate appearance with UV excitation must reflect the population in the $\pi\pi^*$ excited state. The reason for the blueshift of the Auger electrons upon $\pi\pi^*$ excitation can be explained by simulations on the nuclear dynamics of the molecule. These calculations predict that the C-O bond close to the methyl group of thymine [17] stretches in the $\pi\pi^*$ state after UV excitation [4, 5]. The calculated Auger spectrum (Figure 2b) of the $\pi\pi^*$ state with extended C-O bond after initial nuclear relaxation out of the
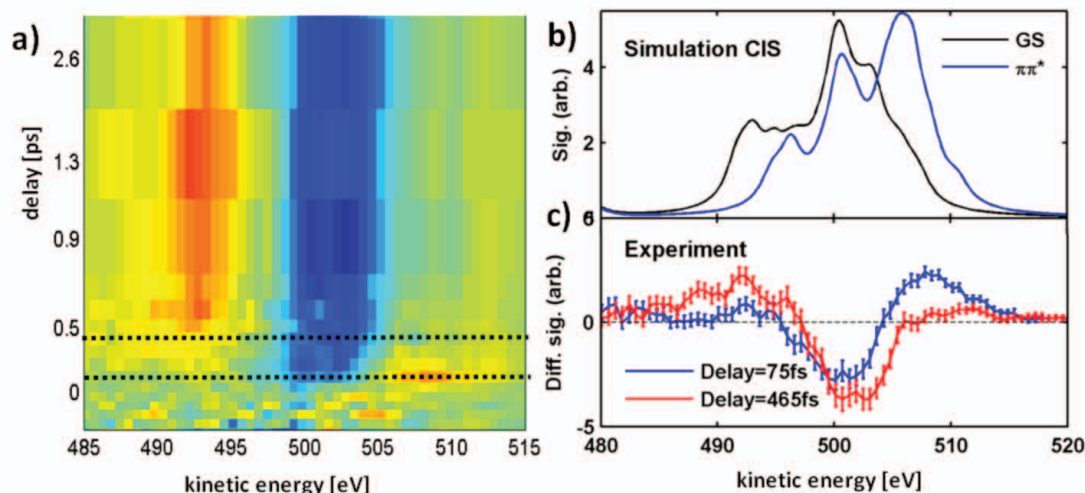
Figure 2: (a) Difference Auger spectrum (excited minus non-excited Auger spectra) as a function of Auger kinetic energy and delay between UV pump and X-ray probe pulse. The false color code indicates UV-enhanced decay (red) and UV-reduced decay (blue). (b) Calculations based on a configuration interaction singles (CIS) model [17] indicate a shift of the Auger spectrum towards higher kinetic energies in the UV-excited ππ* state. (c) The cuts through the difference spectrum at early times clearly exhibit this trend. After around 200 fs, the shift towards higher kinetic energies vanishes and a shift to lower kinetic energies results. © 2014 by Nature Communications. Reproduced with permission from B. K. McFarland et al., Nat. Commun. **5**, 4235 (2014). Permission to reuse must be obtained from the rightsholder.

Franck-Condon region (blue) clearly shows a shift towards higher kinetic energies with respect to the ground-state spectrum (black).

An alternative and intuitive explanation is given using energy conservation arguments in the Auger decay. After Auger decay of the localized O1s hole, the molecule misses two valence electrons, resulting in reduced screening between oxygen and the next nearest carbon. Due to this effect, a strong Coulomb repulsion acts between C and O, which is stored in the molecule at the cost of Auger kinetic energy. If, however, the C-O distance is increased as the C-O bond expands in the ππ* state, less energy is stored in Coulomb repulsion and thus the kinetic energy of the Auger electron increases. This fast C-O nuclear relaxation occurs immediately after the UV excitation, and the experimental time resolution is not high enough to follow the relaxation and resolve the gradual shift.

About 200 fs after photoexcitation, the difference spectrum changes shape. The blue line shape, indicating a shift to higher kinetic energies, has turned into a shape indicating a shift to lower kinetic energies. The dynamics simulations in [4] and [5] predict that the molecule is stuck on a minimum in the ππ* state with extended C-O bond for some picoseconds due to a reaction barrier in the path to reach conical intersections with the ground and nπ*. Thus, these simulations predict a blue-shifted spectrum for the next couple of picoseconds after excitation. The experimentally observed decay of the blue-shifted channel with 200 fs time constant indicates that this minimum can only live for a short time <200 fs. Thus, we find that the majority of the photoexcited ππ* population is not blocked by a barrier and has quick access to the conical intersection region.

Outlook: Future of molecular dynamics probing in the soft X-ray range

Future free electron lasers will provide crucial advantages in two directions: a higher average flux via increased repetition rate and a better control of spectral as well as time domain characteristics of the pulses via seeding techniques.

One of the next FELs to come online, the European XFEL, provides a repetition rate of maximally 27000 Hz. This is accomplished using superconducting accelerator technology, in contrast to the warm copper linear accelerator deployed at LCLS or SACLA. At the European XFEL, the pulses will be delivered in form of 10 Hz macrobunches that can be filled with up to 2700 single bunches, each having a 200 ns delay to the previous one. The flux at the soft X-ray undulator SASE3 is targeted at 10^{18} photons/s [24]. The LCLS II FEL, planned to go online at SLAC National Accelerator Laboratory in 2020, should deliver similar flux with equally spaced pulses up to a repetition rate of 1 MHz. Photon hungry methods such as X-ray photon emission will become feasible at these sources. The 10^7-fold increased flux will lead to 10^4 detected photons from X-ray emission per second under the conditions defined earlier. In addition, the increased repetition rate will, in general, lead to better feedback opportunities. This will most likely be beneficial for synchronization with an optical excitation laser and spectral stability of the X-ray pulse.

Seeded FEL sources provide the preferred path to controlling spectral and temporal pulse parameters. In self-seeding schemes, the SASE output of an undulator section is spectrally filtered and then further amplified in a subsequent undulator. Soft X-ray seeding has been imple-

mented at LCLS, delivering a resolution from 2000–5000 with much higher brightness at the experiment compared to a monochromator after the FEL [25]. This presents a clear advantage for photoelectron spectroscopy. Still, in the case of resonant absorption probing, the spectral pedestals of the typical self-seeded pulse somewhat deteriorate the measured spectra, since the goal is to measure around an edge with steeply increasing absorption cross-section towards the ionization limit.

The FERMI FEL is the first user facility implementing seeding based on high-gain harmonic generation (HGHG), with a conventional ultrafast UV laser as seed [26]. Harmonic lasing of a UV seeded undulator already pushed the spectra into the extreme ultraviolet range. The ultimate goal is to obtain photon energies in the soft X-ray range beyond the carbon K edge at 280 eV [26]. Apart from the obvious advantage of a stable spectrum, the pulse is also closer to the transform limit, as compared to a SASE FEL. In addition, an FEL pulse from HGHG sources is perfectly time-synchronized with the seed laser. This fact can be exploited in molecular pump probe experiments, where the drive laser (or a laser pulse that has the same origin as the drive laser) is exciting the molecular sample.

The past couple of years have also seen a rapid development of smaller, laboratory-based laser high harmonic sources towards shorter wavelength in the soft X-ray region [27–30]. The main technical ad-vancement responsible for this development is mid-infrared ultrafast lasers. The long wavelength used in the harmonic generation process increases the ponderomotive potential for electrons in the HHG process and therefore the cut-off energy of the HHG spectrum. The higher photon energy comes, in principle, at a cost of lower efficiency; however, the gas pressure in the generation region can be increased to compensate for this effect [31]. Harmonic spectra have an extremely broad bandwidth, from the fundamental frequency in the infrared region up to the soft X-ray domain. This characteristic makes the spectrum ideally suited for transient absorption spectroscopy.

In the extreme ultraviolet domain with maximal photon energies below 100 eV, femtosecond and attosecond absorption spectroscopy with harmonic sources is already established [32–34]. One can expect that this type spectroscopy will now be implemented in the SXR range with the tremendous advantage of element sensitivity on carbon, nitrogen, and oxygen. Documented photon numbers of harmonic sources are on the order of 10^7 photons/s in 1% bandwidth at 300 eV with 1 kHz repetition rate [28, 35]. Typical spectral resolution needed for NEXAFS on isolated molecules is 0.25 eV, such that about 10^5–10^6 photons/s are available per spectral bin (given that the spectrometer and detector have low loss). This is sufficient to take high signal-to-noise spectra in a reasonable time. The flux decreases with increasing photon energy

and it will be a matter of compromise between measurement time and noise if higher K-edges like oxygen or even transition metal L-edges become available.

To perform photoelectron spectroscopy, one would need to monochromatize the HHG source, which is not the best way to use a broadband source. The 0.25 eV band with 10^5 photons/s would lead to an emission of 1 electron per 100 seconds if one assumes a typical sample density in PES of 10^{12} cm^{-3}, an absorption cross-section of 1 Mbarn, and an interaction length around 1 mm. This is too low to investigate any excited state features. In the coming years, time-resolved photoelectron spectroscopy will be largely performed at free electron lasers with about five orders of magnitude more photons per second.

Conclusions

Soft X-ray probes provide a new window into the transient dynamics of UV-excited molecules and the transformation of light energy into other degrees of freedom. The element and site sensitivity allows for statements on electronic and geometry changes of particular positions within the molecule. We presented a first experiment on X-ray-induced Auger probing at the oxygen edge of thymine. This was optimally adapted to the strongly fluctuating spectrum of a SASE FEL source.

Future FEL sources promise an extension of X-ray probing towards X-ray absorption, emission, and photoelectron emission techniques. This is mainly due to higher flux at FELs with superconducting accelerators and FEL seeding techniques. High harmonic generation, which is now also covering the soft X-ray range, is ideally suited for X-ray transmission probing. Current published numbers for flux at the carbon K-edge already allow for time-resolved probing.

References

1. W. Domcke, D. Yarkony, and H. Köppel, *Conical Intersections Electronic Structure, Dynamics & Spectroscopy*, World Scientific, Singapore (2004).
2. F. Plasser et al., *Theor. Chem. Acc.* **131**, 233902 (2012).
3. J. C. Tully, *J. Chem. Phys.* **137**, 22A301 (2012).
4. H. R. Hudock et al., *J. Phys. Chem. A* **111**, 8500–8508 (2007).
5. J. J. Szymczak et al., *J. Phys. Chem. A* **113**, 12686–12693 (2009).
6. S. Ullrich et al., *Phys. Chem. Chem. Phys.* **6**, 2796 (2004).
7. H. Tao et al., *J. Chem. Phys.* **134**, 244306 (2011).
8. T. K. Allison et al., *J. Chem. Phys.* **136**, 124317 (2012).
9. M. Assmann, T. Weinacht, and S. Matsika, *J. Chem. Phys.* **144**, 34301 (2016).
10. M. P. Minitti et al., *Phys. Rev. Lett.* **114**, 255501 (2015).
11. J. Küpper et al., *Phys. Rev. Lett.* **112**, 083002 (2014).
12. J. Yang et al., *Nat. Commun.* **7**, 11232 (2016).
13. K. Siegbahn, *ESCA Applied to Free Molecules*, North-Holland, Amsterdam (1969).
14. W. Ackermann et al., *Nat. Photonics* **1**, 336–342 (2007).
15. P. Emma et al., *Nat. Photonics* **4**, 641–647 (2010).
16. T. Ishikawa et al., *Nat. Photonics* **6**, 540–544 (2012).
17. B. K. McFarland et al., *Nat. Commun.* **5**, 4235 (2014).
18. V. S. Petrovic et al., *Phys. Rev. Lett.* **108**, 253006 (2012).
19. B. Erk et al., *Science* **345**, 288–291 (2014).
20. P. Bolognesi et al., *J. Phys. Conf. Ser.* **635**, 112062 (2015).
21. P. Emma et al., *Phys. Rev. Lett.* **92**, 74801 (2004).
22. J. Stöhr, *NEXAFS Spectroscopy*, Springer, Berlin (1996).
23. M. Dell'Angela et al., *Science* **339**, 1302–1305 (2013).
24. S. L. Molodtsov, *Crystallogr. Rep.* **56**, 1217–1223 (2011).
25. D. Ratner et al., *Phys. Rev. Lett.* **114**, 054801 (2015).
26. E. Allaria et al., *Nat. Photonics* **6**, 699–704 (2012).
27. T. Popmintchev et al., *Science* **336**, 1287–1291 (2012).
28. S. L. Cousin et al., *Opt. Lett.* **39**, 5383 (2014).
29. F. Silva et al., *Nat. Commun.* **6**, 6611 (2015).
30. S. M. Teichmann et al., *Nat. Commun.* **7**, 11493 (2016).
31. T. Popmintchev et al., *PNAS* **103**, 13279 (2009).
32. Z.-H. Loh et al., *Phys. Rev. Lett.* **98**, 143601 (2007).
33. E. Goulielmakis et al., *Nature* **466**, 739–743 (2010).
34. C. Ott et al., *Science* **340**, 716–720 (2013).
35. C. Ding et al., *Opt. Express* **22**, 6194 (2014).

SRN 29.6 Focus Topic: Scanning Probe Instruments and Synchrotron Light